

CuO/TiO₂ nanocrystals grown on graphene as visible-light responsive photocatalytic hybrid materials

YUAN FANG¹, RIJING WANG^{1,2}, GUOHUA JIANG^{1,2,*}, HE JIN³, YIN WANG^{1,2}, XINKE SUN^{1,2}, SHENG WANG^{1,2} and TAO WANG^{1,2}

¹College of Materials and Textile, ²Key Laboratory of Advanced Textile Materials and Manufacturing Technology (ATMT), Ministry of Education, ³Qixin Honors College, Zhejiang Sci-Tech University, Hangzhou 310018, P. R. China

MS received 29 March 2011; revised 10 May 2011

Abstract. CuO/TiO₂ nanocrystals grown on graphene (CuO/TiO₂-GR) were prepared by a simple hydrothermal method using Cu(CH₃COO)₂·H₂O and (NH₄)₂TiF₆ as precursors and graphene oxide (GO) as templates. The as-prepared composites were characterized by TEM, XRD, FT-IR to determine composition and phase purity. The photocatalytic activity of the samples was evaluated by photo-degradation of methylene blue (MB) aqueous solution under UV and visible light illumination. This work may provide new insights into preparing other inorganic graphene-based composites.

Keywords. Composite materials; photo-catalyst; electron microscopy; microstructure.

1. Introduction

Graphene is an atomic sheet of *sp*²-bonded carbon atoms owing to its two-dimensional (2D) plate-like structure (Park and Ruoff 2009; He and Gao 2010). Its fascinating physical properties including quantum electronic transport, extremely high mobility, high elasticity, and electromechanical modulation and high surface area make graphene a novel substrate for forming hybrid structures with a variety of nanomaterials (Hsiao *et al* 2010; Akhavan 2010). Future studies require a building block of multifunctional materials as well as structures, because it enables us to exploit versatile and tailor-made properties with performances far beyond those of the individual materials and also opens the door to a wide range of possible applications. One possible way to utilize these properties in applications would be to incorporate graphene sheets hybrids with metals, metal oxides and polymers (Williams *et al* 2008; Pham *et al* 2010; Xiong *et al* 2010). For example, nanohybrids of TiO₂-graphene for improving photocatalytic properties has recently been reported since graphene presents good electron conduction, high surface areas and high adsorption capacities, and they were applied as excellent dopants and supports for TiO₂-based materials to be used as photocatalysts (Williams *et al* 2008; Chen *et al* 2010; Kamegawa *et al* 2010; Liang *et al* 2010; Wang Y *et al* 2010).

Nanocrystal growth on graphene sheets is an important approach to produce nanohybrids, since controlled nucleation and growth affords optimal chemical interactions and

bonding between nanocrystals and graphene sheets, leading to very strong electrical and mechanical coupling within the hybrid. Several methods have been proposed to form nanocrystals on graphene sheets, such as electrochemical deposition (Williams *et al* 2008), sol-gel process (Wang D H *et al* 2010) and gas phase deposition (Wang X R *et al* 2008). In general, it remains a major challenge to develop a facile, one-step solution route for the preparation of inorganic nanostructure composites.

TiO₂ is a very important multifunctional material because of its peculiar and fascinating physicochemical properties and a wide variety of potential uses in diverse fields (Yu *et al* 2008; Ryu and Choi 2008; Jiang and Zeng 2010; Jiang *et al* 2011). However, high energy bandgap of pure TiO₂ ($E_g = 3.0$ eV for rutile, $E_g = 3.2$ eV for anatase) limits its application because the electron-hole pairs can only be formed by UV light at a wavelength shorter than 387 nm (Choi *et al* 1994; Zhou *et al* 2010). In order to improve the solar conversion efficiency, great efforts have been made to extend the useful response of TiO₂-based material to the visible region. Although there are many ways to improve visible light absorption, only very limited cases are reported so far showing significant visible activity, and most systems suffer from rapid charge recombination, the thermal or photochemical instability of the defect materials. It has been reported that CuO and Cu₂O, *p*-type semiconductors, have narrow bandgaps (E_g (CuO) = 1.2 eV and E_g (Cu₂O) = 2.0 eV) (Yu *et al* 2007). CuO has been widely exploited for diverse applications. Herein we demonstrated a facile and reproducible route to obtain a chemically bonded CuO/TiO₂-graphene composite (CuO/TiO₂-GR) via a one-step hydrothermal reaction. The material was found to display an excellent performance in photocatalytic degradation of methylene blue (MB) under visible light.

* Author for correspondence (polymer_jiang@hotmail.com)

2. Experimental

2.1 Materials

Graphite powder (40 μm) was obtained from Qingdao Henglide Graphite Co., Ltd. Concentrated sulfuric acid (H_2SO_4 , 98%), potassium permanganate (KMnO_4) and sodium nitrate (NaNO_3) were purchased from Shanghai Reagents Company and used as received. Cupric acetate ($\text{Cu}(\text{CH}_3\text{COO})_2 \cdot \text{H}_2\text{O}$) and ammonium fluorotitanate ($(\text{NH}_4)_2\text{TiF}_6$) were obtained from Shanghai Chemical Co., Ltd. Methylene blue aqueous solution was prepared by dissolved methylene blue (obtained from Sigma-Aldrich Inc.) in distilled water with concentration (ρ) at 30 mg/L.

2.2 Preparation of $\text{CuO}/\text{TiO}_2\text{-GR}$ composites

First, graphite oxide (GO) was synthesized through graphite powder oxidation with sulfuric acid and potassium permanganate ($\text{H}_2\text{SO}_4\text{-KMnO}_4$) (Pham *et al* 2010). Then, $\text{CuO}/\text{TiO}_2\text{-GR}$ composites were prepared by a one-step hydrothermal reaction. In a typical process, 0.5 g of $\text{Cu}(\text{CH}_3\text{COO})_2 \cdot \text{H}_2\text{O}$ and 1.5 g of $(\text{NH}_4)_2\text{TiF}_6$ were dissolved in 60 mL distilled water to prepare the precursor solution. 0.20 g of GO was added to deionized water (50 mL, in a beaker) and placed in a bath sonicator (125 W) at 80 °C for 2 h to obtain a homogeneous brown solution of GO, followed by introducing the precursor solution. After stirring for 30 min, the mixture was then sealed in a 200 mL Teflon-lined stainless steel autoclave and maintained at 180 °C with a steady stirring. After reaction for 24 h, it was allowed to cool and the solid products were centrifuged and washed three times with water, once with ethanol and then collected and dried under vacuum.

2.3 Characterization

The sizes and morphologies of the resultant samples were characterized by JSM-2100 transmission electron microscopy (TEM) equipped at an accelerating voltage of 200 kV, whereby a small drop of sample solution was deposited onto a carbon-coated copper EM grid (200 mesh) and dried at room temperature at atmospheric pressure. XRD patterns were analysed by using X-ray diffractometer (SIEMENS Diffraktometer D5000, Germany) using $\text{Cu K}\alpha$ radiation source at 35 kV, with a scan rate of 0.02°. Crystallite size of anatase TiO_2 can be determined from the line broadening by using Scherrer's formula. Fourier transform infrared (FT-IR) spectra were recorded on a Nicolet 5700 spectrophotometer using KBr pellets for samples. The UV-Vis spectra were measured by a JASCO V-570 UV/Vis/NiR spectrophotometer (made by JASCO Corporation, Japan).

2.4 Measurement of photocatalytic activity

The photodegradation of methylene blue (MB) dyes was observed based on the absorption spectroscopic technique

(Chen *et al* 2005; Jia *et al* 2009). In a typical process, aqueous solution of MB dyes (0.03 g/L, i.e. 8.1×10^{-5} M, 50 mL) and the photocatalysts (P25 or $\text{CuO}/\text{TiO}_2\text{-GR}$, 30 mg) were placed in a 100 mL cylindrical quartz vessel. Under ambient conditions and stirring, the photoreaction vessel was exposed to UV irradiation produced by a 100 W high pressure Hg lamp with the main wave crest at 365 nm, which was positioned 30 cm away from the vessel (intensity at wavelength of 365 nm at the catalyst mixture surface was 30 $\mu\text{W}/\text{cm}^2$, estimated with a radiometer, Photoelectronic Instrument Co., IPAS). The photocatalytic reaction was started by turning on the Hg lamp, and during the photocatalysis, all other lights were insulated. At given time intervals, the photoreacted solution was analysed by recording variations of the absorption band maximum (660 nm) in the UV-visible spectra of MB. In the visible light photocatalysis, a similar procedure was constructed with a 500 W xenon lamp and a cutoff filter equipped as the light source ($\lambda > 400$ nm, intensity at wavelength of 420 nm at the catalyst mixture surface was 2000 $\mu\text{W}/\text{cm}^2$, estimated with a radiometer, Photoelectronic Instrument Co., IPAS). During photodegradation, the temperature was kept at 20–25 °C and pH of the dispersion was kept at 7.

The ρ_0 was considered as beginning concentration before adding catalyst. The samples were withdrawn regularly from the vessel. The MB concentrations (ρ_i) in different times were obtained and the degradation rate could be expressed as

$$\text{Degradation rate, } R(C/C_0) = (\rho_0 - \rho_i)/\rho_0 \times 100\%.$$

3. Results and discussion

GO upon exfoliation carries sufficient functional groups (e.g. epoxides, hydroxyls, carboxylic acids) to render itself suspendable in polar solvents (Williams *et al* 2008). GO nanosheets are prepared according to a modified Hummer method, resulting in a brown colloidal suspension. The surface morphology of GO is smooth as measured via transmission electron microscopy (TEM), suggesting the formation of a single-layer 2-D nanomaterial (figure 1A). The functional groups on GO provide reactive and anchoring sites for nucleation and growth of nanomaterials (Wang H L *et al* 2010). In the hydrothermal process, fine particles of CuO and TiO_2 (almost amorphous) are firstly coated on GO sheets by hydrolysis of $\text{Cu}(\text{CH}_3\text{COO})_2 \cdot \text{H}_2\text{O}$ and $(\text{NH}_4)_2\text{TiF}_6$. Then, a hydrothermal treatment of the amorphous TiO_2 at 180 °C which led to crystallization of the coating material on GO giving anatase nanocrystals. Electron microscopy images reveal dense CuO/TiO_2 nanocrystals with 30~50 nm in diameter, densely bound to GO sheets, which are not detached even under sonication. The obtained composites retain the two-dimensional sheet structure with micrometers-long wrinkles after hydrothermal reduction.

The composition and phase purity of the as-prepared products are examined by X-ray diffraction (XRD), as shown in figure 2. No diffraction peak of GO (002) is observed at 10.0°

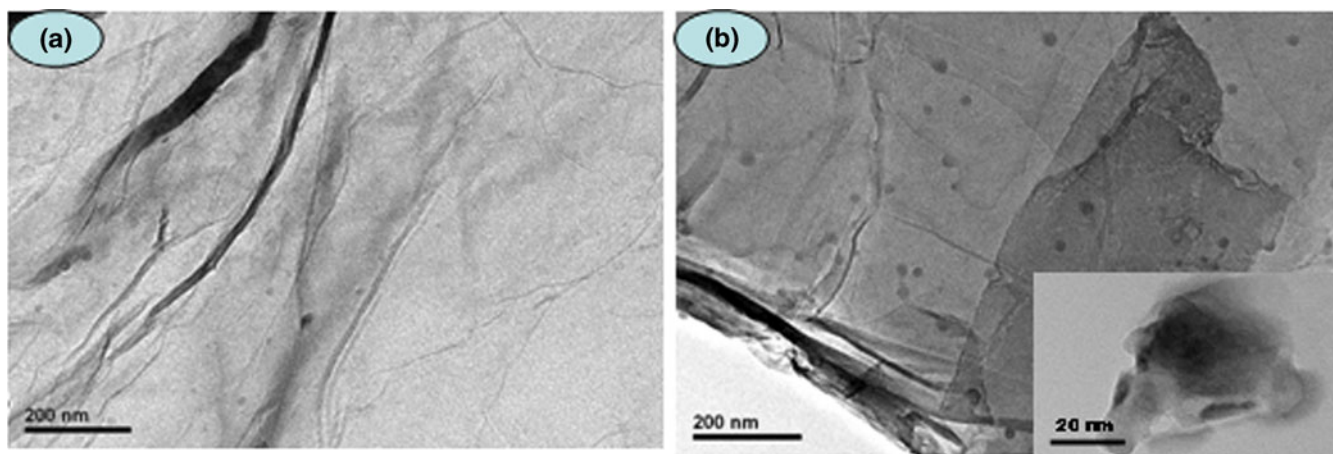


Figure 1. TEM images of graphene (a) and CuO/TiO₂-graphene composites (b).

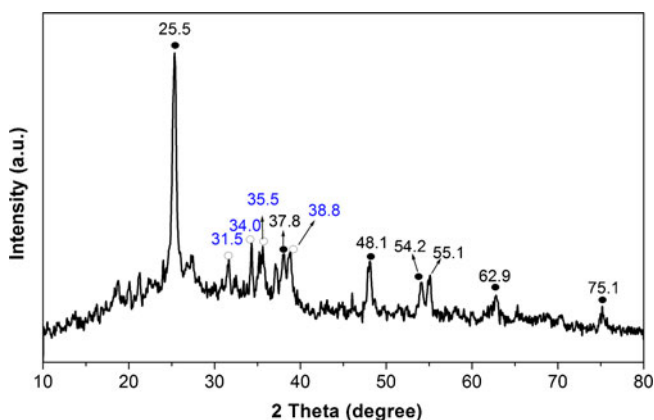


Figure 2. XRD pattern of CuO/TiO₂-graphene composites (hollow circle: anatase TiO₂, solid circle: CuO).

(2θ) (Nethravathi and Rajamathi 2008; Shen *et al* 2009), which indicates that GO has been reduced in the hydrothermal process. The reflection peaks are observed at 2θ values of 25.5, 37.8, 48.1, 54.2, 62.9, and 75.1, which correspond to the anatase structure. It demonstrates that TiO₂ prepared by this method takes the anatase crystalline structure without a significant amount of any other phase. Meanwhile, the reflections of CuO with 2θ values of 31.5, 34.0, 35.5 and 38.8 also can be found in the XRD patterns (Wang J *et al* 2008).

Figure 3 shows FT-IR spectra of GO and as-prepared composites obtained by the hydrothermal process. The broad absorption at low frequency (below 1000 cm⁻¹) is attributed to the vibration of Ti-O-Ti bonds in TiO₂. In fact, this peak can be looked at as a combination of Ti-O-Ti vibration and Ti-O-C vibration (~798 cm⁻¹) (Sakthive and Kisch 2003). The presence of Ti-O-C bonds indicate that during the hydrothermal reduction, graphene oxide, with the residual carboxylic acid functional groups, firmly interact with the surface hydroxyl groups of CuO/TiO₂ hybrid nanoparticles and finally form the chemically bonded composites. The absorption band appearing at ~1600 cm⁻¹ clearly shows the skeletal vibration of the graphene sheets, indicating the

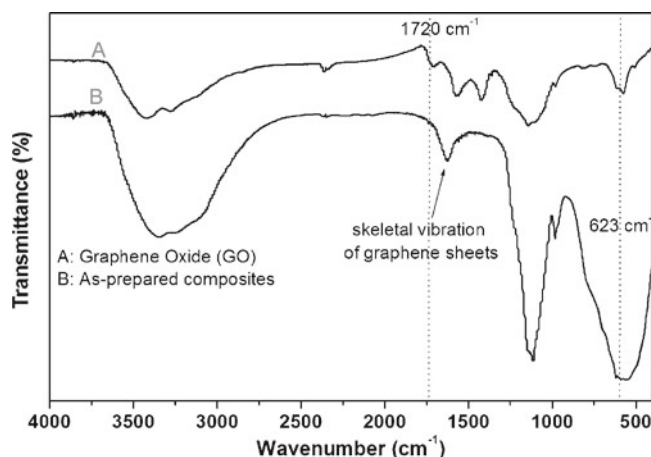


Figure 3. FT-IR spectra of graphene oxide (A) and CuO/TiO₂-GR composites (B).

formation of graphene during the hydrothermal reaction. Besides, in GO, small peak around 1720 cm⁻¹ is assigned to C=O stretching of the residual COOH groups, and the peak disappeared in the composites. The above results confirm the reduction of GO and the combination of CuO/TiO₂ and graphene in the composite. The composite displays a strong absorption peak at around 623 cm⁻¹, which can be attributed to the Cu-O vibration (Zhang *et al* 2006).

The photocatalytic activities of CuO/TiO₂-GR composites are measured by the photodegradation of methylene blue (MB) as model reaction under UV and visible light ($\lambda > 400$ nm), and the results are shown in figure 4. The normalized temporal concentration changes (C/C_0) of MB during the photodegradation are proportional to the normalized maximum absorbance (A/A_0) and derive from the changes in the dye's absorption profile ($\lambda = 660$ nm) at a given time interval. It is clear from figure 4 that the CuO/TiO₂-GR composites show significant progress in the photodegradation of MB compared to P25 (pure TiO₂). Under UV light irradiation, more than 80% of the initial dyes are decomposed

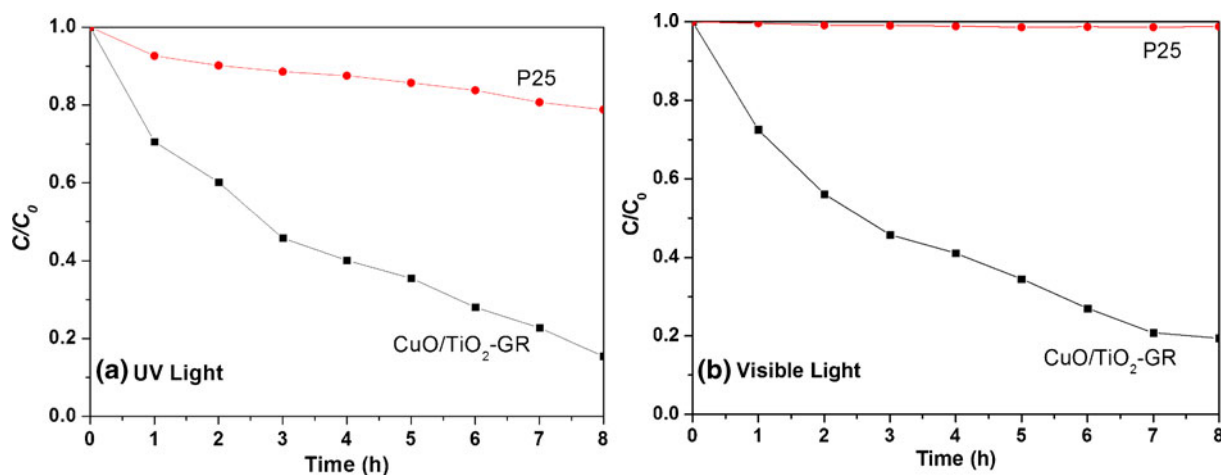


Figure 4. Photodegradation of methylene blue under (a) UV light and (b) visible light ($\lambda > 400$ nm) over P25 and CuO/TiO₂-graphene composites photocatalysts, respectively.

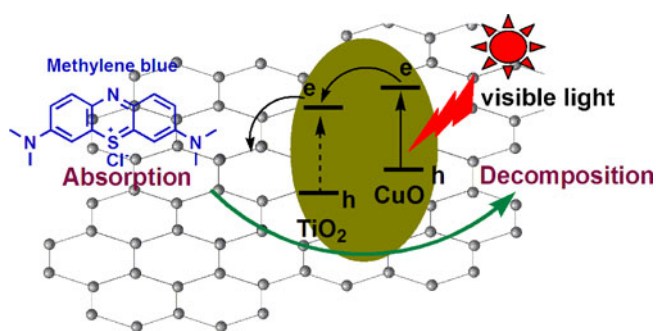


Figure 5. Schematic structure of CuO/TiO₂-GR composites and tentative processes of photodegradation of methylene blue (MB) over CuO/TiO₂-GR composite.

by CuO/TiO₂-GR after around 7 h. Contrastingly, near 80% of the initial dye still remain in the solution after the same time period for bare P25. In addition, in the case of visible light photodegradation, P25 shows rather poor photocatalytic activity due to its limited photoresponding range and only 2% of the initial contaminants diminished after more than 8 h, whereas the CuO/TiO₂-GR composite photocatalyst showed remarkable improvements in the photodegradation rate where 80% of the dye molecules were decomposed after the same time period.

Figure 5 shows schematic structure of CuO/TiO₂-GR composite and tentative processes of the photodegradation of methylene blue (MB) over CuO/TiO₂-GR composite. CuO/TiO₂ nanoparticles are dispersed on the graphene support, and the carbon platform plays an important role during the photodegradation of MB in three aspects: (i) increase catalyst adsorptivity. MB molecules could transfer from the solution to the catalysts' surface and be adsorbed with offset face-to-face orientation via π - π conjugation between MB and aromatic regions of graphene, and therefore, the adsorptivity of dyes increases compared to bare P25, (ii) extend

light absorption. The doping of CuO into the composite renders a red shift in the photoresponding range and facilitates a more efficient utilization of light for the catalyst and (iii) suppress charge recombination. Graphene could act as an acceptor of the photogenerated electrons and ensure fast charge transportation in view of its high conductivity, and therefore, an effective charge separation can be achieved.

4. Conclusions

CuO/TiO₂ nanocrystals grown on graphene oxide (CuO/TiO₂-GR) were prepared in the absence of templates and additives by a simple hydrothermal method using Cu(CH₃COO)₂·H₂O and (NH₄)₂TiF₆ as precursors and graphene oxide (GO) as templates. Because of the functional groups on GO, it provided reactive and anchoring sites for nucleation and growth of nanomaterials and led to CuO/TiO₂ nanocrystals bound to graphene sheets. Because of CuO doping in the composite which led to decreased bandgap energies and visible-light activation, the CuO/TiO₂-GR showed visible light-responsive photo-catalytic property for degradation of methylene blue (MB) aqueous solution under the visible-light illumination. This work may provide new insights into preparing other inorganic hollow microspheres and may extend potential applications for degradation of organic pollutants.

Acknowledgements

This work was financially supported by the Qianjiang Talents Project of Zhejiang Province (2010R10023), the Scientific Research Foundation for the Returned Overseas Chinese Scholars, the State Education Ministry (1001603-C), the Natural Science Foundation of Zhejiang Province (Y4100045, Y4080392, R210101054), the Key Bidding Project of Zhejiang Provincial Key Lab of Fibre Materials and Manufacturing Technology, Zhejiang Sci-Tech University

(S2010002) and the Program for Changjiang Scholars and Innovative Research Team in University (PCSIRT: 0654). One of the authors (HJ) thanks the Xinmiao Talent program of Zhejiang Province for financial support.

References

- Akhavan O 2010 *ACS Nano* **4** 4174
- Chen S H, Chu H Y, Shih Y B and Han C 2005 *J. Vac. Sci. Technol.* **B23** 2557
- Chen C, Cai W, Long M, Zhou B, Wu Y, Wu D and Feng Y 2010 *ACS Nano* **4** 6425
- Choi W, Termin A and Hoffmann M R 1994 *J. Phys. Chem.* **98** 13669
- He H and Gao C 2010 *ACS Appl. Mater. Interfaces* **2** 3201
- Hsiao M C, Liao S H, Yen M Y, Liu P I, Pu N W, Wang C A and Ma C C 2010 *ACS Appl. Mater. Interfaces* **2** 3092
- Jia G, Yang M, Song Y, You H and Zhang H 2009 *Cryst. Growth Des.* **9** 301
- Jiang G and Zeng J 2010 *J. Appl. Polym. Sci.* **116** 779
- Jiang G, Zheng X, Wang Y, Li T and Sun X 2011 *Powder Technol.* **207** 465
- Kamegawa T, Yamahana D and Yamashita H 2010 *J. Phys. Chem.* **C114** 15049
- Liang Y, Wang H, Casalongue H S, Chen Z and Dai H 2010 *Nano Res.* **3** 701
- Nethravathi C and Rajamathi M 2008 *Carbon* **46** 1994
- Park S and Ruoff R S 2009 *Nat. Nanotechnol.* **4** 217
- Pham T A, Kumar N A and Jeong Y T 2010 *Synth. Met.* **160** 2028
- Ryu J and Choi W 2008 *Environ. Sci. Technol.* **42** 294
- Sakthive S and Kisch H 2003 *Angew. Chem. Int. Ed.* **42** 4908
- Shen J, Hu Y, Shi M, Lu X, Qin C, Li C and Ye M 2009 *Chem. Mater.* **21** 3514
- Wang J, Zhang S, Li Z, You J, Yang P, Jiang X and Zhang M 2008 *Bull. Mater. Sci.* **31** 193
- Wang D H *et al* 2010 *ACS Nano* **4** 1587
- Wang H L, Robinson J T, Diankov G and Dai H J 2010 *J. Am. Chem. Soc.* **132** 3270
- Wang X R, Tabakman S M and Dai H J 2008 *J. Am. Chem. Soc.* **130** 8152
- Wang Y, Shi R, Lin J and Zhu Y 2010 *Appl. Catal.* **B100** 179
- Williams G, Seger B and Kamat P 2008 *ACS Nano* **2** 1487
- Xiong Z, Zhang L L, Ma J and Zhao X S 2010 *Chem. Commun.* **46** 6099
- Yu H, Yu J, Liu S and Mann S 2007 *Chem. Mater.* **19** 4327
- Yu J, Liu W and Yu H 2008 *Cryst. Growth Des.* **8** 930
- Zhang Y C, Tang J Y, Wang G L, Zhang M and Hu X Y 2006 *J. Cryst. Growth* **294** 278
- Zhou B, Zhao X, Liu H, Qu J and Huang C P 2010 *Appl. Catal.* **B99** 214